INSTITUTE OF PHYSICS PUBLISHING JOURNAL OF PHYSICS: CONDENSED MATTER

J. Phys.: Condens. Matter **16** (2004) 8387–8398 PII: S0953-8984(04)84491-6

T–P phase diagrams and isotope effects in the Mo–H/D systems

V E Antonov[1,3], **A I Latynin**[1] **and M Tkacz**[2]

[1] Institute of Solid State Physics RAS, 142432 Chernogolovka, Moscow District, Russia
[2] Institute of Physical Chemistry PAS, Kasprzaka 44/52, 01-224 Warsaw, Poland

E-mail: antonov@issp.ac.ru

Received 27 July 2004, in final form 22 October 2004
Published 5 November 2004
Online at stacks.iop.org/JPhysCM/16/8387
doi:10.1088/0953-8984/16/46/024

Abstract

Lines of formation and decomposition of the hcp(ε) molybdenum deuteride in the T–P phase diagram of the Mo–D system are constructed via the measurement of isotherms of the electrical resistance of molybdenum in a deuterium atmosphere at temperatures up to 550 °C and pressures up to 6 GPa. The diagram is compared to that of the Mo–H system studied earlier. The pressure of phase equilibrium in both systems is shown to be much closer to the decomposition pressure than to the formation pressure. A new explanation is suggested for this asymmetry in the hysteresis loop that seems to be characteristic of many metal–hydrogen systems. From the position of the decomposition lines, the standard entropy, enthalpy and Gibbs energy of formation are estimated for molybdenum deuteride and hydride.

1. Introduction

At present, T–P diagrams are constructed for most binary metal–hydrogen systems that form hydrides at hydrogen pressures up to 9 GPa (see review [1] and recent papers [2–5]). In particular, phase transformations in the Mo–H system were studied at pressures of up to 5 GPa and temperatures up to 500 °C using *in situ* resistometry [6] and later up to 1200 °C using *in situ* x-ray diffraction [5]. Phase transformations in metal–deuterium systems at high deuterium pressures are studied to a much lesser extent. The T–P diagram was earlier constructed only for the Ni–D system [7].

The present paper reports on the results of an experimental investigation of the high-pressure T–P diagram of another metal–deuterium system, Mo–D. The effect of substitution of D for H on phase transformations was of special interest in the case of the Mo–H system characterized by a large hysteresis between the curves of formation and decomposition of

[3] Author to whom any correspondence should be addressed.

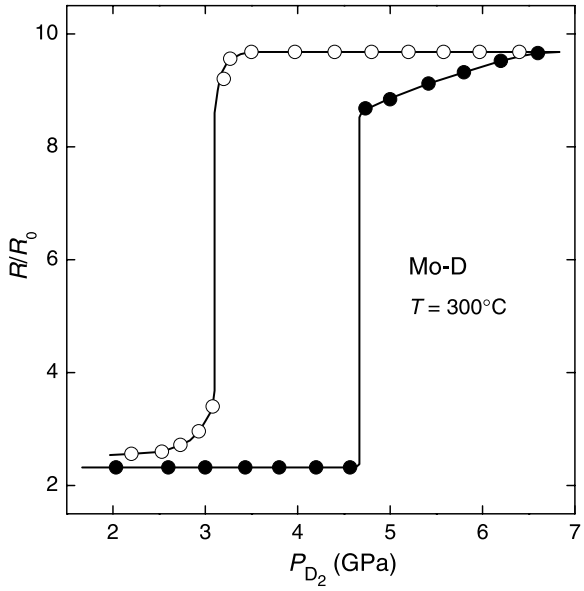

Figure 1. Isotherms of the electrical resistance, R, of molybdenum in a D_2 gas measured at 300 °C in the course of a step-wise increase (solid circles) and decrease (open circles) in pressure. R_0 is the sample resistance under ambient conditions.

the hcp(ε) hydride [6]. This allowed testing the accuracy and applicability of the procedures usually used to derive the equilibrium thermodynamic parameters of high-pressure hydrides from the experimental T–P–c diagrams.

2. Experimental results

The technique used to compress gaseous deuterium to high pressures and to synthesize deuterides is described in [8]. The electrical resistance of Mo in a compressed D_2 gas was measured with samples in the form of strips $3 \times 1 \times 0.05$ mm^3 cut from the same polycrystalline foil of 99.98% molybdenum that had been used in [6] to construct the T–P diagram of the Mo–H system. The resistance was measured by a dc four-probe method with platinum electrodes welded to the sample. The pressure of deuterium was determined with an accuracy of ± 0.3 and ± 0.4 GPa, respectively, in the course of the pressure increase and decrease. The temperature of the sample was measured accurately to within ± 15 °C.

Representative isotherms of the electrical resistance of molybdenum in an atmosphere of molecular deuterium are shown in figure 1. During the measurement, the sample was held at each point until the resistance reached a stationary value and that final value was plotted in the figure. In the intervals of the deuteride formation and decomposition, the resistance drift lasted up to a few hours, which was significantly longer than in the Mo–H system [6] and therefore indicated a slower rate of diffusion processes in the Mo–D system. The Mo–D isotherms looked similar to the Mo–H ones and demonstrated large steps corresponding to the formation and decomposition of the deuteride.

The pressures of formation and decomposition of molybdenum deuteride determined from the midpoints of the steps in the isotherms measured at increasing and decreasing pressure, respectively, are shown in figure 2(a). For comparison, figure 2(b) shows a diagram of the

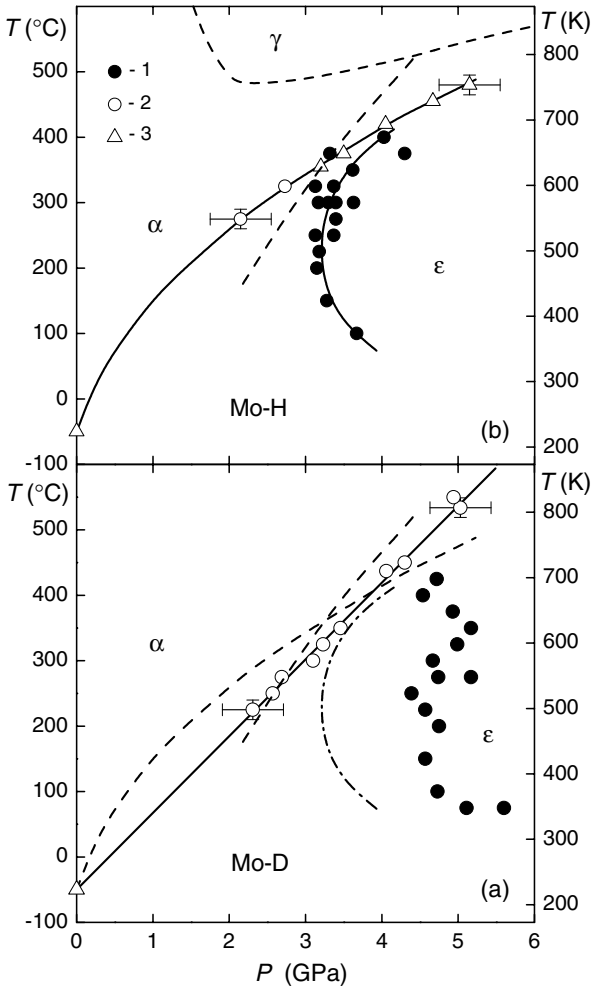

Figure 2. T–P phase diagrams (a) of the Mo–D system (symbols and solid curve, results of the present paper) and (b) of the Mo–H system (symbols and solid curves are for the results of [6], dashed curves of [5]). α is the dilute deuterium or hydrogen solid solution in bcc Mo; ε is the approximately stoichiometric ε-MoD or ε-MoH compound with an hcp metal lattice; γ is the molybdenum hydride with a fcc metal lattice. (1) The $\alpha \rightarrow \varepsilon$ transformation at increasing pressure; (2) the $\varepsilon \rightarrow \alpha$ transformation at decreasing pressure; (3) the $\varepsilon \rightarrow \alpha$ transformation at increasing temperature. The horizontal and vertical bars show the experimental accuracy. The dashed and dash–dotted curves in (a) show the results for ε-MoH taken from (b).

Mo–H system constructed in [6] in a similar way and in [5] using *in situ* x-ray diffraction. The curves of formation and decomposition of molybdenum hydride from figure 2(b) are also plotted in figure 2(a) using broken curves.

As seen from figure 2(b), three different Mo–H phases exist in the studied range of hydrogen pressures and temperatures. These are the α-, ε- and γ-phase with a bcc, hcp and fcc metal lattice, respectively. The triple point of the $(\alpha + \varepsilon + \gamma)$ equilibrium is located at around 4.5 GPa and 500 °C [5]. The solubility of hydrogen in bcc (α) molybdenum remains very small even at high pressures [6, 5]. The ε-phase is molybdenum hydride with a NiAs-type crystal structure, where hydrogen occupies octahedral interstices of the hcp metal lattice [9].

The composition of the ε-hydride is close to the stoichiometry MoH throughout the studied T–P region of its stability [6]. Judging by the lattice parameter of the γ-phase, it is also hydride [5].

The structures and compositions of the α- and ε-phase in the Mo–D system are similar to those in the Mo–H system. The ε deuteride has an hcp metal lattice with virtually the same lattice parameters as the ε hydride [10]. In the present work, we analysed the deuterium content of three Mo–D samples synthesized at a temperature of 325 °C and deuterium pressures of 2.5 GPa (α-phase) and 5 and 7 GPa (ε-phase). Hot extraction gave the atomic ratio D/Mo $< 10^{-3}$ for the sample of the α-phase and D/Mo $= 1.05 \pm 0.03$ for both samples of the ε-phase.

As seen from figure 2, the formation pressures of ε-MoD are significantly higher than those of ε-MoH at temperatures up to about 350 °C. The difference between the decomposition pressures of ε-MoD and ε-MoH does not exceed the experimental error.

3. Discussion

3.1. Hysteresis

Our experiment does not give the pressures P_{eq} of phase equilibrium between the α and ε phase. Instead, we get pairs of the formation and decomposition pressures, P_f and P_d, measured at a given temperature. The problem of localization of P_{eq} inside the interval between P_f and P_d in the metal–hydrogen systems has been debated for many decades, but still remains open. According to one of the concepts, P_{eq} is equidistant from P_f and P_d [11, 12]. According to another, P_{eq} is close to P_d [13–15]. As more and more experimental facts give evidence in favour of the latter concept, it has beome widely accepted in the past few decades. However, no plausible explanation has been advanced so far to account for the difference between the processes occurring in the course of hydride formation and decomposition that makes the hysteresis loop asymmetric. For example, both hydride formation and decomposition were considered as processes of nucleation and growth of a new phase, and P_d was thought to be close to P_{eq} because the decomposition resulted in relaxation of the elastic forces generated on hydrogenation [13]. If this statement were valid, it would be applicable to any phase transformation accompanied by a volume change of the solid. For example, decomposition of a well-relaxed hydride sample should also generate elastic forces, and these forces will relax if the sample is hydrogenated again therefore leading to P_f close to P_{eq}, which is never true.

We think the difference is in the mechanisms of hydride formation and decomposition. Formation of most hydrides starts at the sample surface and the phase boundary moves inside the sample remaining approximately parallel to the surface. Due to the large increase ΔV in the metal volume on hydrogenation, this process necessitates the occurrence of macroscopic fluxes of the material directed outwards and mostly perpendicular to the phase boundary. Generation of such fluxes requires elastic forces of the order of the yield limit of the solid. By contrast, decomposition of most hydrides proceeds via precipitation of hydrogen-depleted particles all over the sample volume that minimizes stresses and strains. Thus, the elastic forces and corresponding elastic deformations generated on hydrogenation should be much larger than those on decomposition, therefore a much larger thermodynamic driving force $\Delta V(P - P_{eq})$ is necessary to compensate for the additional elastic energy in the course of hydride formation. Consequently, the span of the hysteresis loop is mainly determined by the elastic forces arising on hydrogenation and reaching magnitudes of the order of the yield limit of the solid.

So far as high-pressure hydrides are concerned, nickel hydride is studied in more detail and can serve for illustrations. In the course of hydrogenation, the growing layer of this

hydride propagates inside the sample with the interface boundary remaining flat and parallel to the sample surface [16]. On dehydrogenation, the hydrogen-depleted phase is formed by nucleation and growth of particles throughout the sample volume [17].

The occurrence of macroscopic fluxes of the material under hydrogenation can be illustrated by the changes in the geometrical dimensions of Ni rods caused by their hydrogenation and dehydrogenation under high hydrogen pressure [18]. The hydrogenation of a Ni rod about 0.7 mm in diameter and 6 mm long resulted in an approximately equal increase of about 0.055 mm in its diameter and in its length. The rod therefore became thicker by about 8% and longer by only about 1%. After the dehydrogenation, the volume of the rod reverted to the approximately initial value, but the sample got noticeably thicker and shorter.

As indicated in [18], the hydrogenation leads to the approximately equal increase in the diameter, d, and in the length, l, of the Ni rod because by the moment when the boundary of the hydrogenated material moving inwards from the cylindrical surface of the rod reaches its centre, the boundary moving from the end of the rod will have travelled about the same distance $d/2$. As the hydrogenated material mostly flows perpendicular to the boundaries, the thickness of its layer therefore increases by approximately the same *absolute* value both in the radial direction and along the axis of the rod. The dehydrogenation raises no macroscopic flux of the material and results in a nearly uniform decrease in the sample volume thus conserving the new value of the d/l ratio acquired upon the hydrogenation.

Similar irreversible changes in the diameter and length were also observed in the course of hydrogenation and dehydrogenation of Pd rods [19], the effect being apparently of the same origin as in the case of Ni rods [18]. We think therefore that the occurrence of macroscopic fluxes of the material and, correspondingly, of large elastic forces, is an intrinsic property of the hydrogenation process in many metals. Since the character of hydrogenation and dehydrogenation processes in molybdenum is likely to be qualitatively the same as in most other metals, the hysteresis of the $\alpha \leftrightarrow \varepsilon$ transformation in the Mo–H and Mo–D systems should also be determined for the most part by the elastic forces arising on hydrogenation. Consequently, P_{eq} in these systems should be much closer to P_{d} than to P_{f}.

3.2. ΔG^0, ΔS^0 *and* ΔH^0 *derived from experiment*

The accuracy in the determination of P_{d} in the Mo–H and Mo–D systems is comparable with the baric hysteresis of the $\alpha \leftrightarrow \varepsilon$ transformation at temperatures above 200–250 °C (figure 2) and P_{eq} should be much closer to P_{d} than to P_{f}. It is therefore reasonable to assume that $P_{\mathrm{eq}} = P_{\mathrm{d}}$ in this temperature range. Together with the negligibly small H and D solubility in bcc Mo (α-phase) and the nearly invariable composition MoH or MoD of the ε-phase throughout its stability region, this allows a simple thermodynamic analysis of the reactions

$$\mathrm{Mo} + \tfrac{1}{2}\mathrm{H_2} \rightarrow \mathrm{MoH} \qquad \text{and} \qquad \mathrm{Mo} + \tfrac{1}{2}\mathrm{D_2} \rightarrow \mathrm{MoD}.$$

In as much as the Gibbs free energy $\Delta G(P_{\mathrm{eq}}, T) = 0$ for the reaction in equilibrium conditions and $\mathrm{d}G = V\,\mathrm{d}P$ for each phase under isothermal conditions, the value of $\Delta G^0(T)$ reduced to the atmospheric pressure $P_0 = 0.1$ MPa can be calculated as:

$$\Delta G^0_{\mathrm{H}}(T) = \int_{P^{\mathrm{H}}_{\mathrm{eq}}}^{P_0} \Delta V\,\mathrm{d}P = \int_{P^{\mathrm{H}}_{\mathrm{eq}}}^{P_0} (V_{\mathrm{MoH}} - V_{\mathrm{Mo}} - \tfrac{1}{2}V_{\mathrm{H_2}})\,\mathrm{d}P \approx -\beta_{\mathrm{H}} P^{\mathrm{H}}_{\mathrm{eq}} + \tfrac{1}{2}\int_{P_0}^{P^{\mathrm{H}}_{\mathrm{eq}}} V_{\mathrm{H_2}}\,\mathrm{d}P, \quad (1)$$

where $\beta_{\mathrm{H}} = V_{\mathrm{MoH}} - V_{\mathrm{Mo}} \approx 1.3\ \mathrm{cm^3\ mol^{-1}}$ MoH is the partial molar volume of hydrogen in the solid phase [1] nearly independent of pressure and temperature; $V_{\mathrm{H_2}}(P, T)$ is the molar

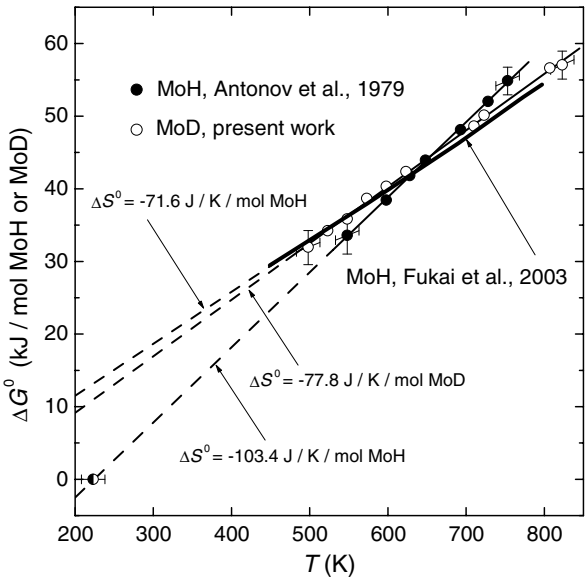

Figure 3. Standard ($P_0 = 0.1$ MPa) free energy $\Delta G^0(T)$ of formation of ε-MoH and ε-MoD.

volume of gaseous hydrogen. The equation for $\Delta G^0_{\mathrm{D}}(T)$ has the same form:

$$\Delta G^0_{\mathrm{D}}(T) = \int_{P^{\mathrm{D}}_{\mathrm{eq}}}^{P_0} \Delta V \,\mathrm{d}P = \int_{P^{\mathrm{D}}_{\mathrm{eq}}}^{P_0} (V_{\mathrm{MoD}} - V_{\mathrm{Mo}} - \tfrac{1}{2}V_{\mathrm{D_2}})\,\mathrm{d}P \approx -\beta_{\mathrm{D}} P^{\mathrm{D}}_{\mathrm{eq}} + \tfrac{1}{2}\int_{P_0}^{P^{\mathrm{D}}_{\mathrm{eq}}} V_{\mathrm{D_2}}\,\mathrm{d}P \quad (2)$$

with $\beta_{\mathrm{D}} \approx \beta_{\mathrm{H}}$ [10].

Figure 3 shows the $\Delta G^0_{\mathrm{H}}(T)$ and $\Delta G^0_{\mathrm{D}}(T)$ dependences calculated using the equations of state of H_2 and D_2 from [20]. The point of decomposition of MoH and MoD at ambient pressure (half-blackened circle) is unlikely to represent equilibrium because the process occurs at a too low temperature of about 220 K. At temperatures exceeding 450 K, each of the three dependences in figure 3 is approximately linear and therefore gives the nearly temperature-independent value

$$\Delta S^0 = -(\partial \Delta G^0/\partial T)_P$$

of the standard (i.e. corresponding to $P = P_0$) entropy of formation of molybdenum hydride and deuteride. The values of ΔS_0 thus obtained are indicated in the figure.

As seen from figure 3, the values of ΔS^0 for MoD from the present work and for MoH from [5] are similar, while ΔS^0 for MoH from [6] is significantly different. The difference between the latter ΔS^0 value and the former two values is rather due to the experimental scatter, because the hydride and deuteride with the same structure and composition should have similar ΔS^0 values (see, e.g., [21] and references therein).

Figure 4 shows dependences of $\Delta G^0/T$ versus $1/T$ constructed using the same calculated values $\Delta G^0_{\mathrm{H}}(T)$ and $\Delta G^0_{\mathrm{D}}(T)$ as in figure 3. Linear interpolation of these dependences at temperatures above 450 K gives the temperature-independent values

$$\Delta H^0 = \left[\frac{\partial(\Delta G^0/T)}{\partial(1/T)}\right]_P$$

of the standard enthalpies of formation of molybdenum hydride and deuteride indicated in the figure. Here again the value for MoH from [6] significantly differs from those for MoH from [5] and for MoD from the present work. Extrapolation of the linear dependences

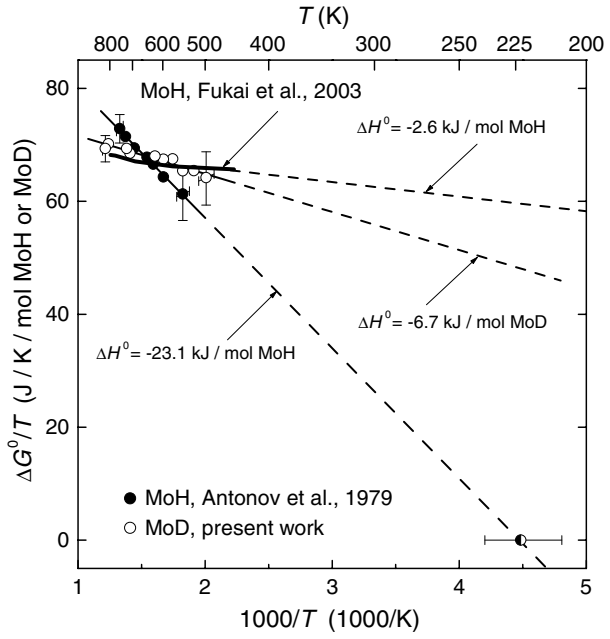

Figure 4. $\Delta G^0(T)/T$ for the Mo–H and Mo–D systems as a function of reciprocal temperature.

$\Delta G^0/T = \Delta H^0/T - \Delta S^0$ shown in figure 4 to $1/T = 0$ gives approximately the same values of ΔS^0 as those derived from the ΔG^0 versus T plots in figure 3.

Figure 5 demonstrates the effect of variation of different terms in equation (2) upon the $\Delta G^0_{\rm D}(T)/T$ versus $1/T$ dependence for the Mo–D system. As seen from comparison of the results depicted by the open circles and solid triangles, the use of the P–V–T relations for gaseous H_2 instead of those for D_2 results in insignificant changes. The total neglect of the increase in the metal volume on deuteration (open squares in figure 5) leads to an approximately 35% overestimation of ΔH^0 and about 15% overestimation of ΔS^0. As the $\beta_{\rm D}$ value is known with relative accuracy better than 10% [10], the inaccuracy in the $\beta_{\rm D} P_{\rm eq}$ term of equation (2) could not therefore noticeably affect the results of the $\Delta G^0_{\rm D}(T)$ calculation.

Similar estimations based on equation (1) show that the changes in the thermodynamic functions of MoH due to the possible inaccuracies of the calculations are also much smaller than those due to the inaccuracy of the determination of $P_{\rm eq}$. This conclusion suggests, in its turn, the low sensitivity of $P_{\rm eq}$ in the Mo–H and Mo–D systems to errors in the calculation of ΔG^0. One could therefore expect that even rough additional thermodynamic estimations would facilitate a more accurate determination of the $\alpha \leftrightarrow \varepsilon$ equilibrium line in the T–P diagrams of these systems.

3.3. Interrelation between $P_{\rm eq}$ in the Mo–H and Mo–D system

The difference $\Delta G^0_{\rm HD}$ between the standard formation energies of MoH and MoD is

$$\Delta G^0_{\rm HD} = \Delta G^0_{\rm H} - \Delta G^0_{\rm D} = (G^0_{\rm MoH} - G^0_{\rm MoD}) - \tfrac{1}{2}(G^0_{\rm H_2} - G^0_{\rm D_2}). \tag{3}$$

The difference $G^0_{\rm H_2} - G^0_{\rm D_2}$ can be calculated using tabulated data of [22], which presents the dissociation energies at $T = 0$ K and the temperature dependences of enthalpy and entropy of gaseous H_2 and D_2 at $P_0 = 0.1$ MPa. In the temperature range of interest, the calculated difference depends on temperature nearly linearly:

$$G^0_{\rm H_2} - G^0_{\rm D_2} \approx 7400 + 14.46T \ [\text{J mol}^{-1}\ \text{H}_2 \text{ and } \text{D}_2]. \tag{4}$$

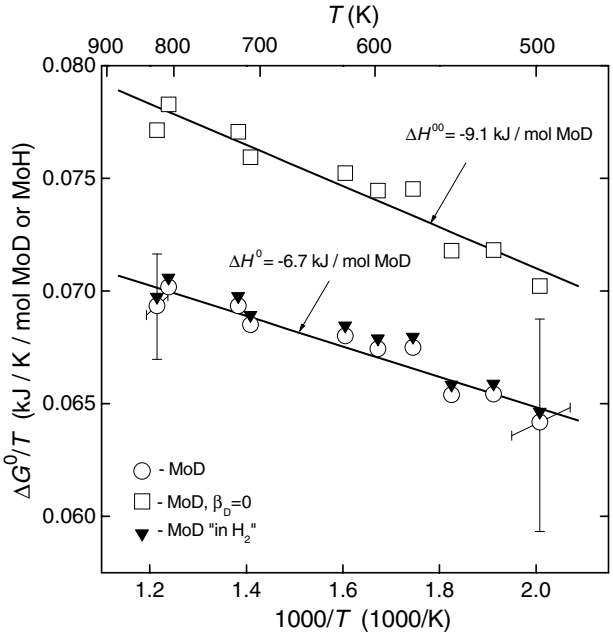

Figure 5. $\Delta G^0(T)/T$ versus $1/T$ dependences for the Mo–D system taken from figure 4 (open circles) and calculated using equation (2) with $\beta_D = 0$ (open squares) or with $V_{H_2}(P, T)$ instead of $V_{D_2}(P, T)$ (solid triangles).

The difference between the free energies of hydride and deuteride of a transition metal is usually assumed to be close to the difference between the free energies of optical vibrations of H and D atoms, the energies being counted from the bottom of the potential well for these atoms in the hydride and deuteride, correspondingly [23]. H and D atoms in the metal are usually considered as three-dimensional Einstein oscillators that gives:

$$G^0_{\mathrm{MoH}} - G^0_{\mathrm{MoD}} \approx 3N_{\mathrm{A}}kT \ln\left[\left(1 - \exp\left(-\frac{\hbar\omega_{\mathrm{H}}}{kT}\right)\right)\Big/\left(1 - \exp\left(-\frac{\hbar\omega_{\mathrm{D}}}{kT}\right)\right)\right] - \frac{3N_{\mathrm{A}}}{2}(\hbar\omega_{\mathrm{H}} - \hbar\omega_{\mathrm{D}}), \tag{5}$$

where $\hbar\omega$ is the energy of the first harmonics, k is the Boltzmann constant and N_{A} is the Avogadro number.

The $\hbar\omega_{\mathrm{H}}$ values of hydrides of most transition metals lie in the range 60–160 meV (see [24] and references therein) and the $\hbar\omega_{\mathrm{D}}$ values of the corresponding deuterides are usually close to $\hbar\omega_{\mathrm{H}}/\sqrt{2}$. The strongest deviation from this harmonic behaviour was found for stoichiometric PdH [25] and PdD [26], which have $\hbar\omega_{\mathrm{H}}/\hbar\omega_{\mathrm{D}} \approx 56$ meV/37 meV ≈ 1.51.

The fundamental band of H optical vibrations in ε-MoH consists of a strong peak at 114 meV with a broad shoulder towards higher energies [27]. The centre of gravity of the band is located at 117 meV, and this value can serve as an estimation of $\hbar\omega_{\mathrm{H}}$ to be used in equation (5). The vibrational spectrum of ε-MoD has not been studied yet, but one can expect that $\hbar\omega_{\mathrm{D}}$ lies somewhere in between the 'ideal' value $\hbar\omega_{\mathrm{H}}/\sqrt{2}$ and the 'anharmonic' value $\hbar\omega_{\mathrm{H}}/1.51$. Most probably, $\hbar\omega_{\mathrm{D}}$ is nearer to $\hbar\omega_{\mathrm{H}}/1.51$ because the superconducting temperature $T_{\mathrm{c}} = 1.11$ K of ε-MoD is higher than $T_{\mathrm{c}} = 0.92$ K of ε-MoH [10] and, by analogy with the Pd–D and Pd–H phases [28], this inverse isotope effect can be attributed to the large anharmonicity in the H vibrations.

Solid curves in figure 6 show the $\Delta G^0_{\mathrm{HD}}(T)$ dependences for MoH/D calculated from equations (3)–(5) using $\hbar\omega_{\mathrm{H}} = 117$ meV and two different values of $\hbar\omega_{\mathrm{D}} = \hbar\omega_{\mathrm{H}}/\sqrt{2}$ and $\hbar\omega_{\mathrm{D}} = \hbar\omega_{\mathrm{H}}/1.51$. Comparison with figure 3 shows that the calculated values of ΔG^0_{HD} are of

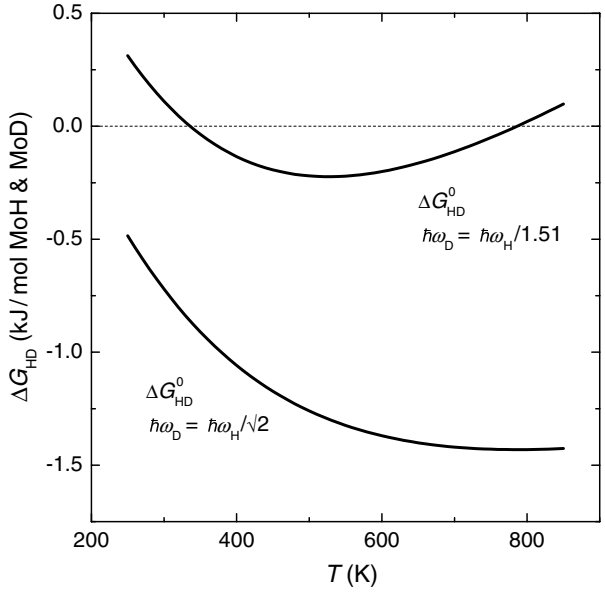

Figure 6. Temperature dependences of $\Delta G^0_{\rm HD} = \Delta G^0_{\rm H} - \Delta G^0_{\rm D}$ for ε-MoH/D calculated from equations (3)–(5) using $\hbar\omega_{\rm H} = 117$ meV and two different values of $\hbar\omega_{\rm D} = \hbar\omega_{\rm H}/\sqrt{2}$ and $\hbar\omega_{\rm D} = \hbar\omega_{\rm H}/1.51$, where $\hbar\omega_{\rm H}$ and $\hbar\omega_{\rm D}$ are the first excitation energies of H and D optical vibrations in ε-MoH and ε-MoD, respectively.

the same order of magnitude as the scatter in the estimations of $\Delta G^0_{\rm H}(T)$ and $\Delta G^0_{\rm D}(T)$. At the same time, one can also see from figure 3 that the arrangement of the ΔG_0 curve of MoD from the present paper and the curve of MoH from [5] is in semiquantitative agreement with the calculated $\Delta G^0_{\rm HD}(T)$ dependences, while the curve for MoH from [6] demonstrates a small, but opposite isotope effect. The interconsistency of the experimental results for MoD [6] and MoH [5] suggests that they represent the $\alpha \leftrightarrow \varepsilon$ equilibrium even more accurately than could be expected from the experimental error.

Additionally, in the case of MoD the experimental $\Delta G^0_{\rm D}/T$ versus $1/T$ dependence in figure 4 and $\Delta G^0_{\rm D}$ versus T dependence in figure 3 demonstrate good linearity and thereby give nearly temperature-independent values of the standard enthalpy and entropy of the reaction over a rather large temperature range, which is a physically reasonable result. We can therefore recommend the obtained values of $\Delta H^0_{\rm D} \approx -7$ kJ mol^{-1} MoD and $\Delta S^0_{\rm D} \approx -80$ J K^{-1} mol^{-1} MoD for reference purposes.

More quantitative estimates of the isotope effect in the Mo–D/H system are possible if one of the obtained temperature dependences of the standard Gibbs energy is assumed to represent the $\alpha \leftrightarrow \varepsilon$ equilibrium. Let it be the dependence for MoD shown by the straight line in figure 4:

$$\Delta G^0_{\rm D,calc}(T)/T = \Delta H^0_{\rm D}/T - \Delta S^0_{\rm D} = -6740/T + 78.3 \ [\text{J K}^{-1}\ \text{mol}^{-1}\ \text{MoD}]. \qquad (6)$$

With $\Delta G^0_{\rm H}(T)$ determined as $\Delta G^0_{\rm H,calc}(T) = \Delta G^0_{\rm D,calc}(T) + \Delta G^0_{\rm HD}(T)$, where $\Delta G^0_{\rm HD}(T)$ is one of the two calculated dependences shown in figure 6, we get two $\Delta G^0_{\rm H,calc}/T$ versus $1/T$ dependences represented in figure 7 by two thin lines. The $\Delta G^0_{\rm H}/T$ versus $1/T$ dependence for the real Mo–H system should lie in between these thin lines. A linear approximation of this dependence at temperatures from 500–800 K gives $\Delta H^0_{\rm H,calc} \approx -7580$ J mol^{-1} MoH and $\Delta S^0_{\rm H,calc} \approx -78.4$ J K^{-1} mol^{-1} MoH.

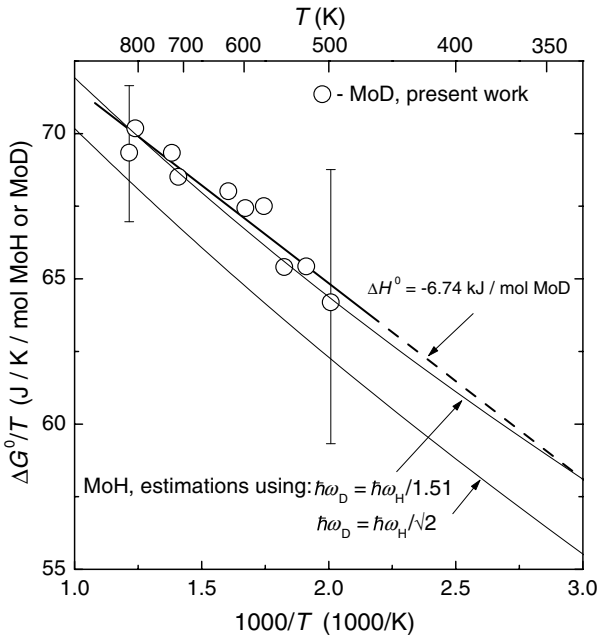

Figure 7. $\Delta G^0(T)/T$ versus $1/T$ dependence for the Mo–D system taken from figure 4 (open circles fitted with the thick straight line given by equation (6)) and two dependences for the Mo–H system (thin solid lines) calculated with $\Delta G^0_{\mathrm{H,calc}}(T) = \Delta G^0_{\mathrm{D,calc}}(T) + \Delta G^0_{\mathrm{HD}}(T)$, where $\Delta G^0_{\mathrm{D,calc}}(T)$ is from equation (6), while $\Delta G^0_{\mathrm{HD}}(T)$ are the two dependences from figure 6.

While the uncertainties in the ΔH^0 and ΔS^0 values for both MoH and MoD are large, the calculated differences $\Delta H^0_{\mathrm{H,calc}} - \Delta H^0_{\mathrm{D,calc}} = -840$ J mol^{-1} MoH and MoD and $\Delta S^0_{\mathrm{H,calc}} - \Delta S^0_{\mathrm{D,calc}} = 0.1$ J K^{-1} mol^{-1} MoH and MoD are much more accurate. We can therefore assume that MoH and MoD have virtually the same standard formation entropies and that the standard formation enthalpy of MoH is about 1 kJ mol^{-1} more negative than that of MoD. As the experimental results for MoD look most reliable, it is reasonable to consider the values of $\Delta H^0_{\mathrm{H}} = \Delta H^0_{\mathrm{D}} - 1 \approx -8$ kJ mol^{-1} MoH and $\Delta S^0_{\mathrm{H}} = \Delta S^0_{\mathrm{D}} \approx -80$ J K^{-1} mol^{-1} MoH as most likely.

Substituting the $\Delta G^0_{\mathrm{D}}(T)$ and $\Delta G^0_{\mathrm{H}}(T)$ dependences shown in figure 7 into equation (2) and (1), respectively, gives the $P^{\mathrm{D}}_{\mathrm{eq}}(T)$ and $P^{\mathrm{H}}_{\mathrm{eq}}(T)$ dependences plotted in figure 8. Similar to figure 7, the curve of the $\alpha \leftrightarrow \varepsilon$ equilibrium in the Mo–H system is expected to lie in figure 8 between the two thin solid curves.

4. Conclusions

The large hysteresis of the $\alpha \leftrightarrow \varepsilon$ transformation in the Mo–H system is still greater in the Mo–D system due to the lower diffusion rate of D in Mo. Experiment showed that the formation pressures of ε-MoD are significantly higher than those of ε-MoH at temperatures up to about 350 °C, while the difference between the decomposition pressures of ε-MoD and ε-MoH does not exceed the experimental error. This evidences that the pressure of the $\alpha \leftrightarrow \varepsilon$ equilibrium in both Mo–H and Mo–D system is much closer to the decomposition pressure than to the formation pressure, because the lines of the $\alpha \leftrightarrow \varepsilon$ equilibrium in the T–P diagrams of these

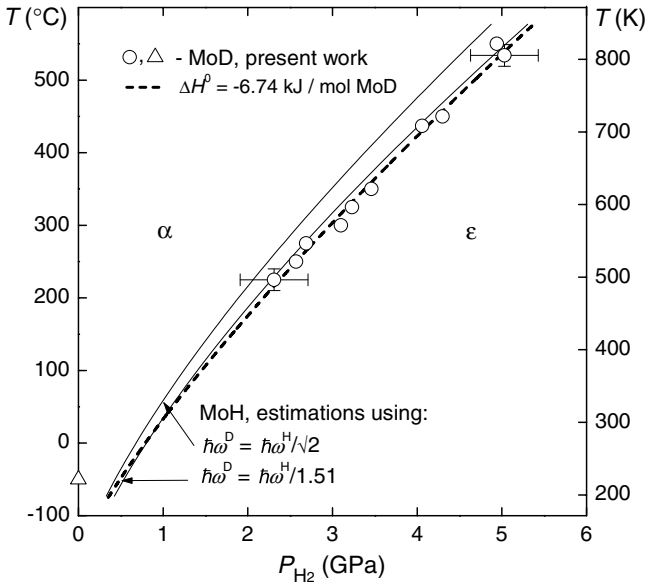

Figure 8. Most plausible curves of the $\alpha \leftrightarrow \varepsilon$ equilibrium (see text) in the Mo–D system (thick dashed curve) and in the Mo–H system (two thin solid curves) together with the experimental values of decomposition pressure of ε-MoD (open symbols).

systems should be close to each other owing to the specific value $\hbar\omega_{\mathrm{H}} \approx 117$ meV of the hydrogen optical modes in ε-MoH.

It is widely believed that similar asymmetry in the hysteresis loop is typical of many metal–hydrogen systems. No plausible explanation has however been advanced so far to account for the difference between the processes occurring in the course of hydride formation and decomposition that makes the hysteresis loop asymmetric. We think the difference is in the mechanisms of hydride formation and decomposition. Formation of most hydrides starts at the sample surface and the phase boundary moves inside the sample remaining approximately parallel to the surface. Due to the large increase in the metal volume on hydrogenation, this process necessitates the occurrence of macroscopic fluxes of the material directed outwards and mostly perpendicular to the phase boundary. Generation of such fluxes requires elastic forces of the order of the yield limit of the solid. By contrast, decomposition of most hydrides proceeds via precipitation of hydrogen-depleted particles all over the sample volume that minimizes stresses and strains. Thus, these are the elastic forces arising on hydrogenation that mainly determine the span of the hysteresis loop.

At temperatures from 200–550 °C, the difference between the equilibrium pressures in the Mo–H and Mo–D system estimated with $\hbar\omega_{\mathrm{H}} \approx 117$ meV does not exceed the experimental error of a few tenths of gigapascal in the evaluation of the hydride or deuteride decomposition pressure. It is therefore reasonable to assume that the equilibrium pressure is equal to the decomposition pressure, as is often done in the case of metal–hydrogen systems. This approximation, however, does not result in a reliable evaluation of the standard thermodynamic parameters of ε-MoH and ε-MoD from the position of the decomposition lines, because the lines are not determined accurate enough for such a procedure. A simple comparative analysis of thermodynamic properties of the Mo–H and Mo–D system allows a considerable improvement of the accuracy of the evaluation. The recommended values of the standard

enthalpy ΔH^0, entropy ΔS^0 and the Gibbs energy $\Delta G^0 = \Delta H^0 - T\Delta S^0$ under normal conditions are:

$\Delta H^0_{\mathrm{H}} \approx -8$ kJ mol^{-1} MoH, $\Delta S^0_{\mathrm{H}} \approx -80$ J K^{-1} mol^{-1} MoH, $\Delta G^0_{\mathrm{H}} \approx +16$ kJ mol^{-1} MoH;
$\Delta H^0_{\mathrm{D}} \approx -7$ kJ mol^{-1} MoD, $\Delta S^0_{\mathrm{D}} \approx -80$ J K^{-1} mol^{-1} MoD, $\Delta G^0_{\mathrm{D}} \approx +17$ kJ mol^{-1} MoD.

Acknowledgments

This work was supported by grant no 02-02-16859 from the Russian Foundation for Basic Research and by the Joint Project 'Hydrogen Energy' of the Russian Academy of Sciences and MMC Norilsk Nickel.

References

[1] Antonov V E 2002 *J. Alloys Compounds* **330–332** 110–6
[2] Fukai Y and Mizutani M 2002 *Mater. Trans.* **43** 1079–84
[3] Fukai Y, Haraguchi T, Shinomiya H and Mori K 2002 *Scr. Mater.* **46** 679–84
[4] Fukai Y, Mori K and Shinomiya H 2003 *J. Alloys Compounds* **348** 105–9
[5] Fukai Y and Mizutani M 2003 *Mater. Trans.* **44** 1359–62
[6] Antonov V E, Belash I T and Ponyatovskii E G 1979 *Dokl. Akad. Nauk SSSR* **248** 635–7 (in Russian)
[7] Antonov V E, Belash I T and Ponyatovskii E G 1977 *Dokl. Akad. Nauk SSSR* **233** 1114–7 (in Russian)
[8] Antonov V E, Belash I T, Belyashova A I, Zatsepina N N, Latynin A I and Chirin N A 1989 *Fiz. Tekh. Vysok. Davlenii* **31** 12–5 (in Russian)
[9] Irodova A V, Glazkov V P, Somenkov V A, Shil'shtein S Sh, Antonov V E and Ponyatovskii E G 1988 *Kristallografiya* **33** 769–71
Irodova A V, Glazkov V P, Somenkov V A, Shil'shtein S Sh, Antonov V E and Ponyatovskii E G 1988 *Sov. Phys.—Crystallogr.* **33** 453–5 (Engl. Transl.)
[10] Antonov V E, Belash I T, Zharikov O V, Latynin A I and Palnichenko A V 1988 *Fiz. Tverd. Tela* **30** 598–600
Antonov V E, Belash I T, Zharikov O V, Latynin A I and Palnichenko A V 1988 *Sov. Phys.—Solid State* **30** 344–5 (Engl. Transl.)
[11] Wagner C 1944 *Z. Phys. Chem* **193** 386–406
[12] Flanagan T B and Clewley J D 1982 *J. Less-Common Met.* **83** 127–41
[13] Scholtus N A and Hall W K 1963 *J. Chem. Phys.* **39** 868–70
[14] Baranowski B and Bocheńska K 1965 *Z. Phys. Chem. NF* **45** 140–52
[15] Wicke E and Blaurock J 1987 *J. Less-Common Met.* **130** 351–63
[16] Bauer H J and Jonitz D 1969 *Z. Angew. Phys.* **28** 40–3
[17] Jonitz D and Bauer H J 1978 *Z. Naturf.* a **33** 1599–600
[18] Antonov V E, Belash I T and Ponyatovskii E G 1984 *Dokl. Akad. Nauk SSSR* **278** 892–6 (in Russian)
[19] Lewis F A 1982 *Platinum Met. Rev.* **26** 70–8
[20] Tkacz M and Litwiniuk A 2002 *J. Alloys Compounds* **330–332** 89–92
[21] Lässer R and Klatt K-H 1983 *Phys. Rev.* B **28** 748–58
[22] *Themodynamical Properties of Individual Substances: a Handbook* 1962 (Moscow: Izd. Akad. Nauk SSSR) (in Russian)
[23] Wicke E and Brodowsky H 1978 *Hydrogen in Metals II* (*Springer Topics in Applied Physics* vol 29) ed G Alefeld and J Völkl (Berlin: Springer) pp 72–155
[24] Antonov V E, Cornell K, Dorner B, Fedotov V K, Grosse G, Kolesnikov A I, Wagner F E and Wipf H 2000 *Solid State Commun.* **113** 569–72
[25] Ross D K, Antonov V E, Bokhenkov E L, Kolesnikov A I, Ponyatovsky E G and Tomkinson J 1998 *Phys. Rev.* B **58** 2591–5
[26] Kolesnikov A I, Antonov V E, Fedotov V K, Grosse G, Ivanov A S and Wagner F E 2002 *Physica* B **316/317** 158–61
[27] Dorner B, Belash I T, Bokhenkov E L, Ponyatovsky E G, Antonov V E and Pronina L N 1989 *Solid State Commun.* **69** 121–4
[28] Ganguly B N 1973 *Z. Phys.* **265** 433–9
Ganguly B N 1973 *Phys. Lett.* A **46** 23–4